Biofabrication

International Society for Biofabrication

PAPER • **OPEN ACCESS**

A novel technique for the production of electrospun scaffolds with tailored three-dimensional micro-patterns employing additive manufacturing

To cite this article: Catherine M Rogers *et al* 2014 *Biofabrication* **6** 035003

View the article online for updates and enhancements.

Related content

- A novel electrospun biphasic scaffold provides optimal three-dimensional topography for in vitro co-culture of airway epithelial and fibroblast cells
G E Morris, J C Bridge, L A Brace et al.
- Electrospun fiber scaffolds of poly (glycerol-dodecanedioate) and its gelatin blended polymers for soft tissue engineering
Xizi Dai, Khadija Kathiria and Yen-Chih Huang
- Multiscale fabrication of biomimetic scaffolds for tympanic membrane tissue engineering
Carlos Mota, Serena Danti, Delfo D'Alessandro et al.

Recent citations

- Bio-functional electrospun nanomaterials: From topology design to biological applications
Jinpeng Han *et al*
- Micro-/Nano-Scales Direct Cell Behavior on Biomaterial Surfaces
Shuo Wang *et al*
- Luciano P. Silva

This content was downloaded from IP address 128.243.44.244 on 27/03/2019 at 20:56

OPEN ACCESS
IOP Publishing
Biofabrication

Biofabrication **6** (2014) 035003 (11pp)
doi:10.1088/1758-5082/6/3/035003

A novel technique for the production of electrospun scaffolds with tailored three-dimensional micro-patterns employing additive manufacturing

Catherine M Rogers[1], **Gavin E Morris**[1], **Toby W A Gould**[1], **Robert Bail**[2], **Sotiria Toumpaniari**[1], **Helen Harrington**[1], **James E Dixon**[1], **Kevin M Shakesheff**[1], **Joel Segal**[2] **and Felicity R A J Rose**[1]

[1] Division of Drug Delivery and Tissue Engineering, Centre for Biomolecular Sciences, School of Pharmacy, University of Nottingham, Nottingham, NG7 2RD, UK
[2] Manufacturing Research Division, Faculty of Engineering, University of Nottingham, Nottingham, NG7 2RD, UK

E-mail: felicity.rose@nottingham.ac.uk

Received 16 September 2013, revised 25 February 2014
Accepted for publication 10 March 2014
Published 11 April 2014

Abstract

Electrospinning is a common technique used to fabricate fibrous scaffolds for tissue engineering applications. There is now growing interest in assessing the ability of collector plate design to influence the patterning of the fibres during the electrospinning process. In this study, we investigate a novel method to generate hybrid electrospun scaffolds consisting of both random fibres and a defined three-dimensional (3D) micro-topography at the surface, using patterned resin formers produced by rapid prototyping (RP). Poly(D,L-lactide-co-glycolide) was electrospun onto the engineered RP surfaces and the ability of these formers to influence microfibre patterning in the resulting scaffolds visualized by scanning electron microscopy. Electrospun scaffolds with patterns mirroring the microstructures of the formers were successfully fabricated. The effect of the resulting fibre patterns and 3D geometries on mammalian cell adhesion and proliferation was investigated by seeding enhanced green fluorescent protein labelled 3T3 fibroblasts onto the scaffolds. Following 24 h and four days of culture, the seeded scaffolds were visually assessed by confocal macro- and microscopy. The patterning of the fibres guided initial cell adhesion to the scaffold with subsequent proliferation over the geometry resulting in the cells being held in a 3D micro-topography. Such patterning could be designed to replicate a specific *in vivo* structure; we use the dermal papillae as an exemplar here. In conclusion, a novel, versatile and scalable method to produce hybrid electrospun scaffolds has been developed. The 3D directional cues of the patterned fibres have been shown to influence cell behaviour and could be used to culture cells within a similar 3D micro-topography as experienced *in vivo*.

Keywords: electrospinning, rapid prototyping, additive manufacturing, 3D geometry, cell adhesion

(Some figures may appear in colour only in the online journal)

Content from this work may be used under the terms of the Creative Commons Attribution 3.0 licence. Any further distribution of this work must maintain attribution to the author(s) and the title of the work, journal citation and DOI.

Introduction

The selection and fabrication of the appropriate scaffold is a crucial factor in tissue engineering to promote *in vivo*-like cell behaviour. As such, the three-dimensional (3D) architecture of the artificial extracellular matrix (ECM) is important in governing the eventual structural and mechanical properties of the engineered tissue (Vats *et al* 2003).

Electrospinning is a technique used widely to fabricate micro- and nano-fibrous scaffolds that mimic the native ECM environment to various degrees (Xin *et al* 2007, Vaquette and Cooper-White 2011, Zhang *et al* 2009, Brun *et al* 2011, van Aalst *et al* 2008). During the electrospinning process, the fibres collect on two-dimensional (2D) plates, resulting in scaffolds composed of consecutive layers of randomly arranged fibrous sheets (Zhang and Chang 2008). As it is known that specific architectures can promote favourable biological responses, such as enhanced cell attachment, proliferation and differentiation, cell–cell signalling and ECM deposition, there is significant interest in controlling the spatial arrangement of electrospun fibres to generate patterned structures (Wu *et al* 2010).

A number of experimental approaches to produce electrospun scaffolds consisting of aligned fibres have since been identified, including the application of either an external magnetic or electric fields or by using rotating metallic mandrels or metal rings as collectors (Yang *et al* 2007, Li *et al* 2003, Xie *et al* 2010). New variants of electrospinning such as near-field and polymer melt have recently been designed, which improve the control of fibre arrangement in resultant scaffolds (Chang *et al* 2008, Teo *et al* 2011, Lyons *et al* 2004). In the first of these new approaches, the distance between the needle tip and collector is reduced and in the second variant, the increased viscosity of polymer melts stabilizes the spinning jet (Chang *et al* 2008, Teo *et al* 2011, Lyons *et al* 2004). A number of research groups have since adapted these novel electrospinning variants with fast motion automated collecting systems resulting in direct writing methods (Lee *et al* 2012, Brown *et al* 2011, Bisht *et al* 2011). The electrospun scaffolds produced by these writing methods have precise architectures and patterns (Lee *et al* 2012, Brown *et al* 2011, Bisht *et al* 2011). The main drawbacks with these new electrospinning approaches are that they are relatively slow experimental techniques and opportunities to scale-up manufacture of patterned scaffolds using these methods could be limited.

Recent studies have begun to identify new collector plate designs to generate electrospun scaffolds with ordered 3D fibrous structures (Vaquette and Cooper-White 2011, Zhang *et al* 2009, Zhang and Chang 2007, 2008, Li *et al* 2003, 2004, 2005). Li *et al* (2005) have shown that fibres unaxially align when insulated regions are introduced on the collector plates and Vaquette and Cooper-White (2011) have demonstrated that the patterns introduced onto stainless steel collector plates by attaching wire meshes or drilling structures were accurately mimicked in their resultant electrospun scaffolds. Despite these advances, the challenge to identify a reproducible, flexible and scalable method to design and manufacture collector plates with precisely controlled structures remains. Therefore, there is now great interest in converging additive manufacturing (AM) approaches with electrospinning (Dalton *et al* 2013). AM produces complex 3D structures in a layer-by-layer process by computer aided design (CAD) and hence has the potential to produce collector plates with accurately controlled geometries for electrospinning (Dalton *et al* 2013).

In this study, we have combined an AM approach with electrospinning to design novel collector geometries that when placed on the collector plate and electrospun onto, produced hybrid scaffolds consisting of both random fibres and a defined 3D micro-topography at the surface. A rapid prototyping (RP) system was employed to design and manufacture the patterned resin formers (collectors). This AM approach provides a precise, robust, versatile and scalable means of fabricating formers with precisely controlled microgeometries. The RP formers can be manufactured according to the specific requirements of the end-user and hence could be designed to closely mimic the topography of native tissues. In this study, various former designs were manufactured with feature sizes ranging from 100–1000 μm and the ability of the resulting patterned 3D electrospun poly(D,L-lactide-co-glycolide) (PLGA) scaffolds to influence *in vitro* 3T3 fibroblast cell adhesion and proliferation was investigated. Initially we assessed the adaptability of the process in terms of the patterning that could be reproduced using this method and then focussed on a design that replicated the dimensions of the undulating 3D micro-topography of the dermal papillae as an exemplar.

Table 1. A summary of the former designs and dimensions produced.

Pattern	Width (μm)	Height (μm)	Length (μm)
Sinusoidal	1000	1000	–
Sinusoidal	1000	500	–
Sinusoidal	500	1000	–
Saw-tooth	300	300	–
Hexagonal	400	300	–
Reentrant honeycomb	1000	100	500

Materials and methods

Former design and manufacture

CADs of a range of former geometries from a simple sinusoidal wave to a more complex re-entrant honeycomb (exhibits negative Poisson's ratio) were created (table 1). The CAD models were then uploaded to the Perfactory® Mini-Multi Lens machine (EnvisionTEC, Gladbeck, Germany). This 3D RP system uses a projection-microstereolithography method to generate the patterned resin (R11 Acrylate resin; EnvisionTEC, Gladbeck, Germany) formers in a layer-by-layer AM process. The Perfactory uses a digital micro-mirror device combined with a light projector to solidify the liquid photo-curable resin formers (each layer is 25 μm thick) into the required 3D patterns. The manufactured RP resin formers were then sputter coated with a thin layer of gold (Balzers Union

Table 2. Mechanical properties of the electrospun scaffolds.

Pattern	Width (μm)	Height (μm)	Stretch direction to wave	Maximum stress (MPa)	Young's modulus (MPa)
Sinusoidal	1000	1000	Parallel	0.42 ± 0.07	9.05 ± 0.97
Sinusoidal	1000	1000	Perpendicular	0.54 ± 0.11	10.41 ± 0.41
Sinusoidal	1000	500	Parallel	0.43 ± 0.12	11.93 ± 2.47
Sinusoidal	1000	500	Perpendicular	0.43 ± 0.06	7.33 ± 2.88
Sinusoidal	500	1000	Parallel	0.73 ± 0.12	14.91 ± 1.93
Sinusoidal	500	1000	Perpendicular	1.01 ± 0.07	18.42 ± 6.39
Random	–	–	–	0.63 ± 0.04	11.65 ± 2.07

SCD 030, Balzers Union Ltd, Liechtenstein), as the surface of electrospinning collectors must be electroconductive in order to collect fibres (Reneker and Chun 1996, Bellan and Craighead 2006).

Electrospun scaffold fabrication

Commercially available PLGA (75:25) (Lakeshore Biomaterials, Birmingham, Alabama, USA) was dissolved in dichloromethane (DCM; Fisher Scientific, Loughborough, UK) to produce a 15% (w/w) solution and loaded into a 10 mL syringe (BD Falcon™, Oxford, UK) with a blunt 18-gauge (G) needle (BD Falcon™, Oxford, UK) attached. The syringe was then placed in a syringe pump driver (Harvard Apparatus Ltd, Kent, UK) set at a solution feed rate of 4 mL h^{-1}. A voltage was applied (19 kV) and the fibres collected onto the target RP patterned formers (mounted on a steel collector plate) positioned 20 cm from the needle tip. The electrospinning procedure was conducted at room temperature within a vented chemical fume hood.

Cell culture

Murine 3T3 fibroblast cells were obtained from the European Collection of Cell Cultures (ECACC, UK) and cultured in 75 cm^2 flasks (Nunc™, Fisher Scientific, Loughborough, UK) in Dulbecco's modified Eagle's medium (DMEM; Invitrogen, Paisley, UK) supplemented with 10% (v/v) foetal calf serum (FCS; Sigma-Aldrich Company Ltd, Dorset, UK), 2 mM L-glutamine solution (Sigma-Aldrich Company Ltd, Dorset, UK) and 1% (v/v) antibiotic/antimycotic solution (10 000 units mL^{-1} penicillin G, 100 mg mL^{-1} streptomycin sulphate and 25 μg mL^{-1} amphotericin B; Sigma-Aldrich Company Ltd, Dorset, UK). The medium was changed twice a week, with all cultures maintained in a humidified environment at 37 °C, 5% CO_2 in air. The cells were genetically labelled using transduction of lentiviruses expressing enhanced green fluorescent protein (eGFP) as previously described (Dixon *et al* 2011).

Bright-field microscopy

The 3D profiles of the manufactured resin RP formers and the resulting patterned electrospun scaffolds were visualized in bright-field using an inverted microscope (Leica MM IRBE; Leica Microsystems Ltd, Milton Keynes, UK) and digital images were captured using the associated QCapture software (QImaging, Leica Microsystems Ltd, Milton Keynes, UK).

Mechanical properties

The mechanical properties of three different sinusoidal scaffolds (table 2) were assessed using a dynamic mechanical analyser (DMA, Q800; TA Instruments, Elstree, UK). Uniaxial tensile tests established the effect of different geometries on the overall scaffold strength in both the parallel and perpendicular directions to the sinusoidal waves ($n = 3$ for each) whilst randomly orientated scaffolds produced on the steel collector plate were employed as controls. Scaffolds were cut into 15 mm × 10 mm rectangles, loaded onto the DMA and incubated at 37 °C. A force ramp rate of 0.5 N min^{-1}, with an upper force limit of 1 N, was then applied to generate stress/strain curves. From these curves, the maximum stress (MPa), at which the scaffolds failed (tore), and the Young's modulus (MPa; at 2.5% strain) was determined for each scaffold type.

Cell-seeded PLGA constructs

The sinusoidal PLGA scaffolds (5 mm disks) were placed in a non-tissue culture treated 96-well plate (BD Falcon™, Oxford, UK), ultraviolet (UV) sterilized (30 min exposure time) and pre-wetted with DMEM. eGFP-labelled 3T3 fibroblasts were trypsinized (trypsin solution 25 g L^{-1} in 0.9% (w/v) sodium chloride, ethylenediaminetetracetic acid solution 0.02% (w/v) in distilled water (dH_2O); Sigma-Aldrich Company Ltd, Dorset, UK), counted and seeded (8×10^4 cells) separately onto the scaffolds. The 3T3-seeded constructs were cultured as described above for up to four days. Randomly orientated scaffolds were seeded as controls.

Scanning electron microscopy and subsequent image analysis

The architectural properties of the fabricated patterned PLGA scaffolds were observed using scanning electron microscopy (SEM; JEOL JMS-6060 LV, JEOL Ltd, Welwyn Garden City, Hertfordshire, UK). The scaffolds were sputter coated with a thin layer of gold (Balzers Union SCD 030, Balzers Union Ltd, Liechtenstein) before being imaged with the associated Smile View program (JEOL Ltd, Welwyn Garden City, Hertfordshire, UK). To assess 3T3 fibroblast proliferation on the patterned scaffolds, the cell-seeded constructs were removed from day 4 of culture, washed three times in phosphate buffered saline (PBS; Oxoid Ltd, Hampshire, UK) and fixed in 3% (w/v) glutaraldehydye solution (Sigma-Aldrich Company Ltd, Dorset, UK) overnight at 4 °C.

The cell-seeded constructs were washed three times in dH_2O, dehydrated through a series of ethanol (25, 50, 70, 90, 95 and 100% in dH_2O; Fisher Scientific, Loughborough, UK) and air-dried overnight in an externally vented fume hood. Cell seeded-constructs were coated with a thin layer of gold before being imaged with the Smile View program as described previously. Image analysis of fibre diameter was conducted using ImageJ 1.47v. Measurements were taken from the SEM images in the regions of interest highlighted in figure 4. Working from left to right, fibre diameters were measured until at least 50 measurements were taken; averaged data ± standard deviation (SD) were determined.

Fluorescence confocal macroscopy and microscopy

Prior to imaging, the cell-seeded constructs were removed from culture, washed three times in PBS and fixed in 10% (w/v) formalin solution (Sigma-Aldrich Company Ltd, Dorset, UK). Confocal macroscopy was used to assess both the overall geometry of the patterned scaffolds and 3T3 fibroblast adhesion to the microfibres. Following 24 h culture, fluorescence macroconfocal images (Leica TCS LSI, Leica Microsystems Ltd, Milton Keynes, UK) of the PLGA fibres (reflectance, excitation 515–560 nm, emission 590 nm) and adherent cells (eGFP, excitation 450–90 nm, emission 515 nm) were taken. Confocal microscopy was employed to establish the 3D profile of the patterned scaffolds and cell proliferation over the constructs. The seeded constructs from day 4 of culture were mounted with 'ProLong® Gold Antifade reagent with DAPI (4,6-Diamidino-2-phenylindole; Invitrogen™, Paisley, UK) to visualize the cell nuclei. Fluorescence microconfocal images (Leica TCS SP2, Leica Microsystems Ltd, Milton Keynes, UK) of the cell populations on the patterned scaffolds (DAPI, excitation 340–80 nm, emission 425 nm and eGFP, excitation 450–90 nm, emission 515 nm) were taken.

Alamar Blue® assay for cell viability

The Alamar Blue® assay (Serotec, Kidlington, UK) was used to assess the number of viable 3T3 fibroblasts after four days culture on the sinusoidal scaffolds. The cell-seeded constructs were transferred to a non-tissue culture treated 24-well plate (BD Falcon™, Oxford, UK) and washed three times with phosphate buffered saline (PBS, Sigma-Aldrich®, Dorset, UK). The membranes were then incubated with 1 mL of Alamar Blue® working solution for 90 min at 37 °C, 5% CO_2 in air. Following this time, triplicate 100 μL aliquots were removed from each well and placed in a black 96-well assay plate (BD Falcon™, Oxford, UK). Fluorescence was measured using the excitation filters at 530 and 590 nm (multimode microplate reader, Infinite® 200 Pro Series; Tecan Ltd, Reading, UK) respectively, to determine the total number of viable cells attached to the scaffolds after four days of culture. A standard curve of viable cell number versus fluorescence intensity was created from dilutions of a 5×10^5 cell suspension. Randomly orientated scaffolds were used as controls and non-seeded constructs were employed as blanks in this experiment.

Statistical analysis

All experiments were performed in triplicate unless otherwise stated in the figure legend. The mean ± standard error of mean or standard deviation values of all data was calculated as indicated in the figure legend. The statistical significance of results was assessed using either an unpaired t test (figure 4) or a one-way analysis of variance (ANOVA) with a Tukey–Kramer multiple comparisons test (figure 7) or with a Kruskal–Wallis post-test (table 2) using GraphPad Instat version 3.0 (GraphPad Software Inc., CA, USA). To determine if the differences in the means of the fibre diameters (figure 4) measured from the peak or the valley sections of the scaffolds were significant the unpaired t test was used as the samples were taken by measuring two independent populations of fibres (peak and valley; see figure 4). The sample sets were also of unequal size although >50 measurements were taken in all cases enabling us to make the assumption that the means are normally distributed and that the population variances, although unknown, were equal. Data presented in table 2 were analysed using the non-parametric Dunn ANOVA test due to the small sample size ($n = 3$); a Kruskal–Wallis post-test was selected but not calculated because the P value was greater than 0.05 and therefore considered not significant. Results were considered significant when $p < 0.05$ (*), very significant when $p < 0.01$ (**), highly significant when $p < 0.001$ (***) and extremely significant when $p < 0.0001$ (****).

Results

Former manufacture

CAD models of the desired sinusoidal, saw-toothed, hexagonal and re-entrant honeycomb former geometries were created (figures 1(*A*), 3(*A*), (*C*) and (*E*)) and uploaded to the Perfactory® system to produce the precise micro-patterned resin RP formers. Bright-field microscopic images of the patterned RP formers showed their resulting 3D profiles (figures 1(*B*), 3(*B*), (*D*) and (*F*)).

Electrospun scaffold fabrication

PLGA microfibres were electrospun onto the manufactured resin RP formers. Bright-field microscopic images showed that the resulting scaffolds had well organized topological structures, when both dense and sparse fibre mats were electrospun, and SEM images provided more details on the patterning of the microfibres (figures 1(*C*) and (*D*)). Sinusoidal electrospun PLGA scaffolds consisting of patterns with a range of dimensions from 500–1000 μm (reflecting measurements of the dermal papillae as determined from histology sections) were generated from their respective RP formers (figures 1(*D*) and 2). SEM images revealed that each of the resulting scaffolds mirrored the patterning of the manufactured formers. At the apex of the sinusoidal waves, compact layers of microfibres were present. The spacing and width of these fibre bundles varied according to the wavelength of their corresponding RP former geometry. The remaining areas of these sinusoidal scaffolds were found to consist of randomly orientated PLGA microfibres.

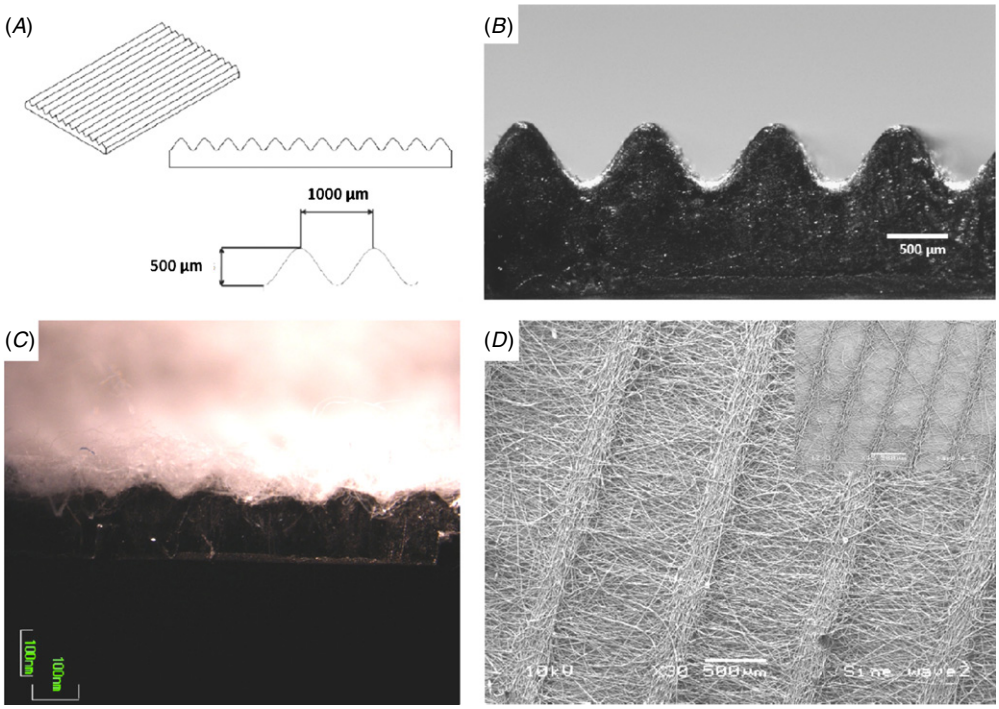

Figure 1. The design and manufacture of patterned formers and the resulting electrospun scaffolds. Representative images of a sinusoidal CAD model (*A*), the resultant RP resin former (*B*), electrospun PLGA fibres collected on the former and the subsequent patterned scaffold (*D*). This patterning was transferred to the scaffolds when both dense (*D*) and sparse (*D*) (inset) fibre mats were electrospun.

A similar pattern of densely packed patterned fibres and randomly orientated microfibres was seen when using the saw-tooth RP former with a smaller 3D profile of 300 μm $\times$ 300 μm (figure 3(*B*)). No apparent difference between the resulting scaffold morphology was observed for those scaffolds collected onto saw-toothed or sinusoidal designed RP formers.

Both the shapes and dimensions of more complex 3D hexagonal and re-entrant honeycomb RP formers were closely mirrored in the resulting electrospun scaffolds (figures 3(*D*) and (*F*)). SEM images of these tailored scaffolds showed that the outline of both these intricate patterns consisted of densely packed areas of patterned PLGA microfibers with the remaining regions of the scaffolds comprised of randomly arranged fibres.

Fibre diameter analysis

Fibre diameter analysis revealed that the diameters of the fibres of the sinusoidal and sawtooth electrospun mats were similar (figures 4(*A*)–(*D*)). Fibre diameters of fibres found in the peak regions of the sinusoidal scaffolds were on average 7.9 μm compared with 8.2 μm for the sawtooth design. Comparing fibre diameters of those present in the valley regions revealed average fibre diameters of 7.5 and 6.8 μm for the sinusoidal and sawtooth scaffolds respectively. Statistical analysis revealed that there was no statistical significant difference between fibre diameters of fibres present in the peak and valley regions of the sinusoidal scaffold. In contrast, fibre diameters were highly significantly different between those present in the peak and valley regions of the sawtooth design ($p < 0.001$).

There was no significant difference between the diameters of the fibres present in the two areas of the hexagonal patterned scaffold with average fibre diameters of 4.7 and 4.3 μm in the peak and valley regions respectively (figures 4(*E*) and (*G*)). However, the greatest difference in fibre diameters within a single scaffold design were found in the re-entrant honeycomb electrospun scaffolds (figures 4(*F*) and (*H*)). Fibres with average diameters of 2.1 μm were present in the peak region, whilst those in the valley averaged 4.7 μm; this was found to be extremely significantly different ($p = 0.0001$).

Mechanical strength

The mechanical strength of the three different sized sinusoidal scaffolds and randomly orientated fibre scaffold was assessed using a DMA (table 2). There was no significance difference in the maximum stress or Young's modulus between the randomly orientated and the three sinusoidal scaffolds when tested in the parallel or perpendicular direction.

Cell adhesion and proliferation

Fluorescence macroconfocal imaging of the overall 3D geometry of the patterned constructs confirmed previous observations from the SEM in that the resultant scaffolds mirrored the sinusoidal geometries of the RP formers (figure 5(*A*)). Scaffolds with sinusoidal geometries were seeded with cells and 24 h later, macroconfocal imaging revealed that eGFP-labelled 3T3 cells had preferentially adhered to the patterned PLGA microfibre regions of the sinusoidal waves (figures 5(*B*) and (*C*)). This patterning of cell adhesion on the sinusoidal scaffolds was confirmed

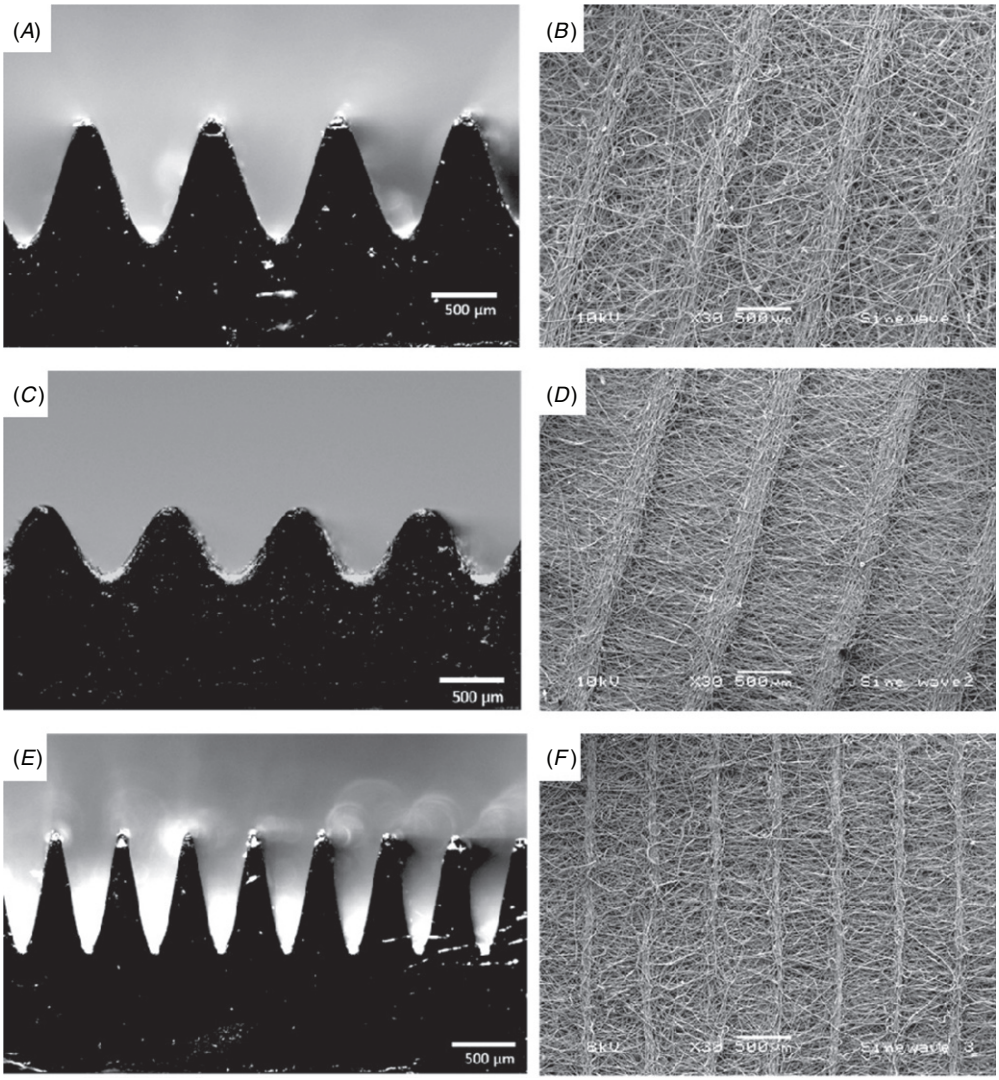

Figure 2. The manufactured sinusoidal RP resin formers and the resulting electrospun PLGA scaffolds. Representative images of the 1000 μm $\times$ 1000 μm (wavelength $\times$ height) (*A*) and (*B*), 1000 μm $\times$ 500 μm (*C*) and (*D*) and 500 μm $\times$ 1000 μm (*E*) and (*F*) formers and scaffolds produced.

in corresponding low magnification fluorescence images (figures 5(*D*) and (*E*)). Cell adhesion on the hexagonal patterned scaffold was also seen to be influenced by the fibre pattern (figures 5(*F*) and (*G*)). Fluorescence confocal microscopy confirmed that the mammalian cells had proliferated over the 3D sinusoidal waves of the scaffolds by day 4 and were held in the overall 3D undulating shape of the scaffold (figures 6(*A*) and (*B*)). Along with SEM observations, the fluorescence microconfocal images also showed that the 3T3 cells had reached confluency on the patterned constructs following this culture period (figure 6(*C*)).

Cell viability

The Alamar Blue® assay was employed to determine the effect of scaffold patterning on *in vitro* cell viability. No significant difference was seen in the number of viable 3T3 cells present on the sinusoidal compared to the control scaffolds (random fibres) over the four day culture period, indicating that culturing cells on the patterned geometries was not detrimental to cell viability (figure 7). Wave height appeared to influence viability, as fewer viable cells were present on the shorter 500 μm sinusoidal pattern compared to the two higher 1000 μm scaffolds. This difference in viability was significant ($p < 0.05$) between the 1000 μm $\times$ 1000 μm and 500 μm $\times$ 1000 μm geometries.

Discussion

The present study is the first to demonstrate the ability to fabricate hybrid electrospun scaffolds with both random and controlled 3D micro-patterns using collector plates produced by an AM approach. To our knowledge, no other study has reported fabricating patterned electrospun scaffolds using such RP formers. This versatile, flexible and scalable AM method has the capability of producing a wide variety of formers with closely controlled microfeatures and hence has the potential to manufacture electrospun scaffolds with any required 3D architecture (Dalton *et al* 2013).

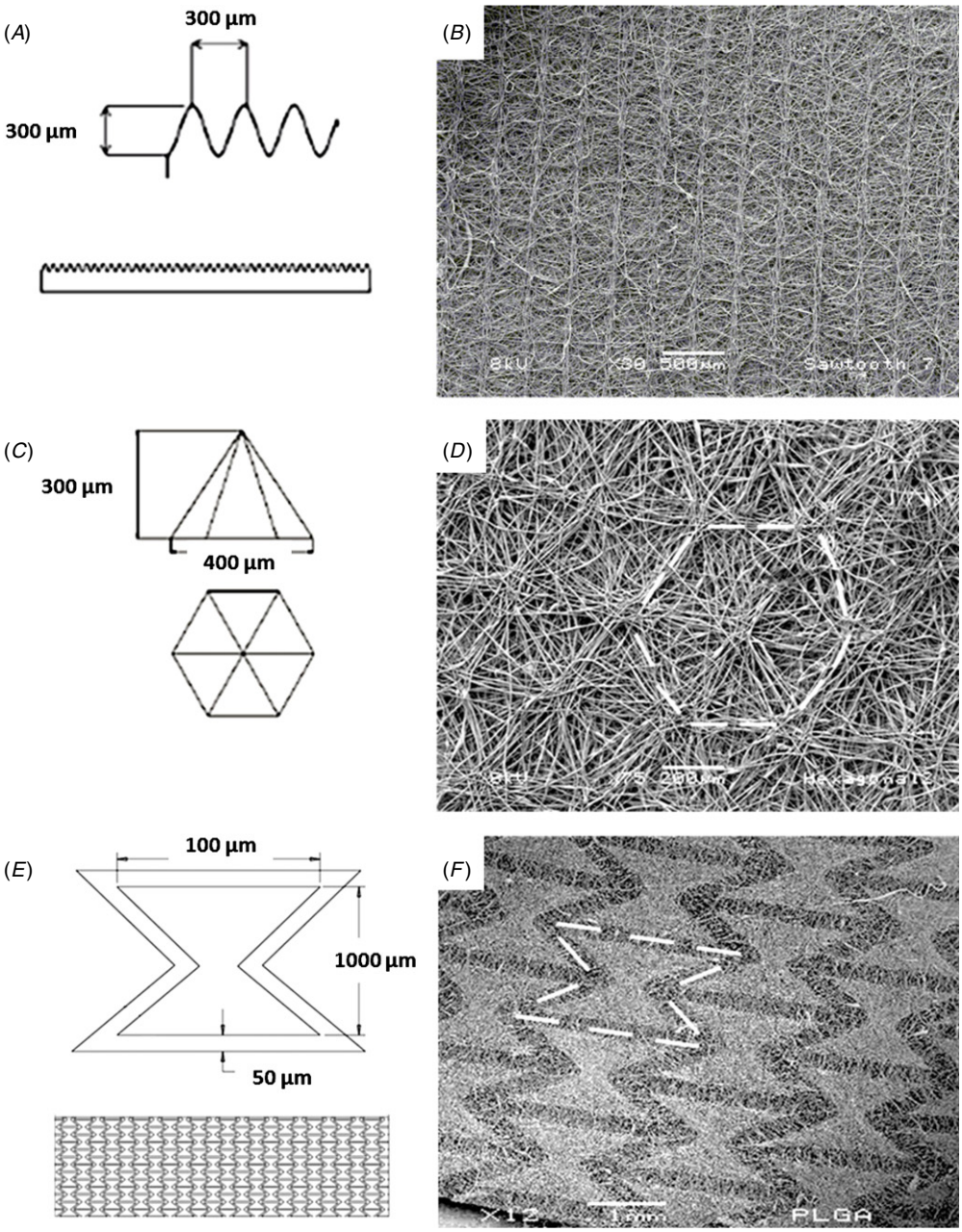

Figure 3. The versatility of the RP approach to produce formers with various 3D geometries and the resulting patterned scaffolds. Representative images of the sawtooth (*A*) and (*B*), hexagonal (*C*) and (*D*), and re-entrant honeycomb (*E*) and (*F*) CAD models and electrospun scaffolds.

During this study, a number of former geometries were designed and fabricated using the Envisiontec Perfactory™ RP system. PLGA fibres were successfully electrospun onto the patterned formers and both SEM and confocal macroscopy images confirmed that the resultant patterned fibrous scaffolds mirrored the geometries and dimensions of all the 3D designs investigated, thus illustrating the versatility of this technique. The PLGA microfibres were attracted to the apexes of both the sinusoidal and saw-toothed formers and to the sidelines of the more complex hexagonal and re-entrant honeycomb patterns, resulting in dense areas of patterned fibres. The remaining sections of these scaffolds consisted of fewer randomly orientated fibres. Fibre diameter analysis revealed that the fibres found in the different regions of the patterns were of similar diameter for the sinusoidal and hexagonal designs. In contrast, fibre diameters of the saw-tooth and re-entrant honeycomb designs were significantly different when comparing the peak and valley regions within the same scaffold. Interestingly, the re-entrant honeycomb design was the only geometry where the fibre diameters in the valley were greater than those in the peak regions. This indicates that the geometry of the former not only influences where the electrospun fibre eventually comes to rest on the former but that it can also influence fibre diameter within a single design without alteration to the electrospinning conditions. This phenomenon warrants further investigation to fully understand

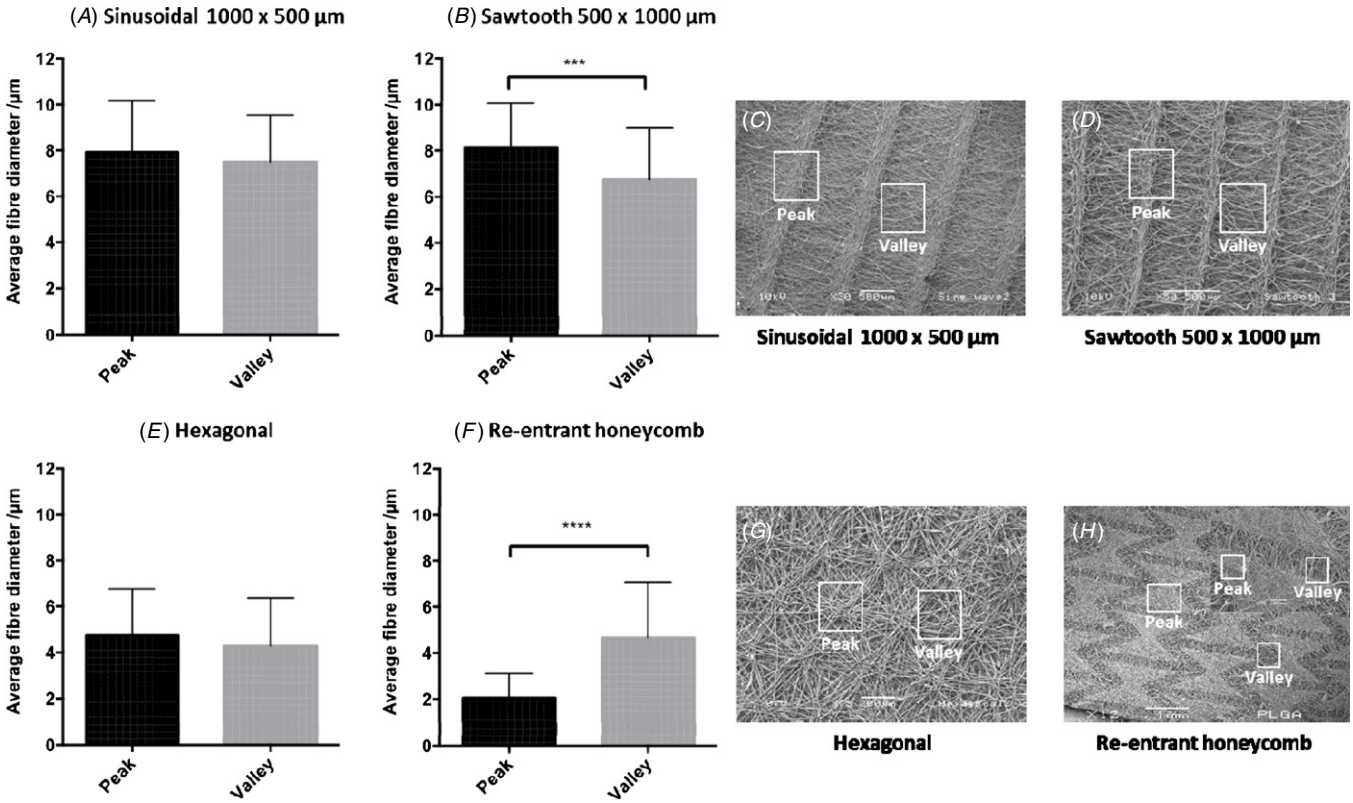

Figure 4. Fibre diameter analysis of the fibre based scaffolds with varying 3D geometry ((*A*) sinusoidal 1000 μm $\times$ 500 μm, (*B*) sawtooth 500 μm $\times$ 1000 μm; (*E*) hexagonal and (*F*) re-entrant honeycomb). Error bars represent SD; *** $p < 0.001$, **** $p < 0.0001$ (a minimum of 50 fibre diameter measurements were taken for each dataset). Representative scanning electron micrograph images of each of the 3D geometries analysed ((*C*) sinusoidal 1000 μm $\times$ 500 μm, (*D*) sawtooth 500 μm $\times$ 1000 μm; (*G*) hexagonal and (*H*) re-entrant honeycomb including high magnification inset). Fibre diameter measurements were taken from both the 'peak' and 'valley' regions of the 3D patterns as indicated on each image (white box).

to what extent fibre patterning and fibre diameter can be influenced using this method.

Mechanical testing of the sinusoidal scaffolds was carried out to provide an initial indication of the influence of the various 3D patterns on the mechanical properties of the scaffolds. Preliminary data illustrated that this patterning did not significantly influence scaffold strength confirming that the pattern was solely a surface topographical feature. It has been previously reported that the height differences in areas of patterned collector plates and hence distances to the needle tips influenced the fibre orientation, density and diameter (Zhang and Chang 2008). Further work from our laboratories has used the RP technique reported here to produce similar patterned electrospun scaffolds using poly(ethylene terephthalate) (PET), illustrating that this method is transferable to other polymers (data not shown).

A number of collector plate designs including those consisting of steel plates with pre-drilled holes, electroconductive wire meshes, plastic plates covered by a metallic needle matrix and a thread crest of a screw have recently been developed by researchers to investigate their influence on fibre arrangement in electrospun scaffolds (Vaquette and Cooper-White 2011, Zhang *et al* 2009, Li *et al* 2003, 2004, 2005, Zhang and Chang 2007, Neves *et al* 2007). Vaquette and Cooper-White (2011) have examined the ability of patterned collectors to increase scaffold porosity and hence enhance *in vitro* cell infiltration into the electrospun scaffolds. Using patterned scaffolds produced from a screw and wired mesh, Neves *et al* (2007) have shown that cells adhere to and adapt their shape according to the local topography. The main limitations with these current methods are the lack of versatility, reproducibility and scalability in the design and manufacture of the patterned collectors. In our study, we have demonstrated a novel method to fabricate electrospun scaffolds with tailored geometries from collector plates that have been produced using a precise, robust, flexible and scalable AM approach.

As topography influences cellular response, patterned scaffolds that closely replicate the native microgeometry of tissues is of great interest in the development of *in vitro* models for studying diseases and screening potential therapeutics (Neves *et al* 2007, Rim *et al* 2013, Guex *et al* 2013, Kaiser *et al* 2006, Curtis and Wilkinson 1997). In this study, we investigated the influence of the sinusoidal electrospun scaffolds that closely mimic not only the fibrous nature of the ECM but also the native 3D undulating geometry of the dermal papillae, on *in vitro* mammalian cell adhesion, viability and proliferation. This undulating structure is important as it supports the dermal stem cell niche and hence influences stem cell localization and migration; the dimensions of this

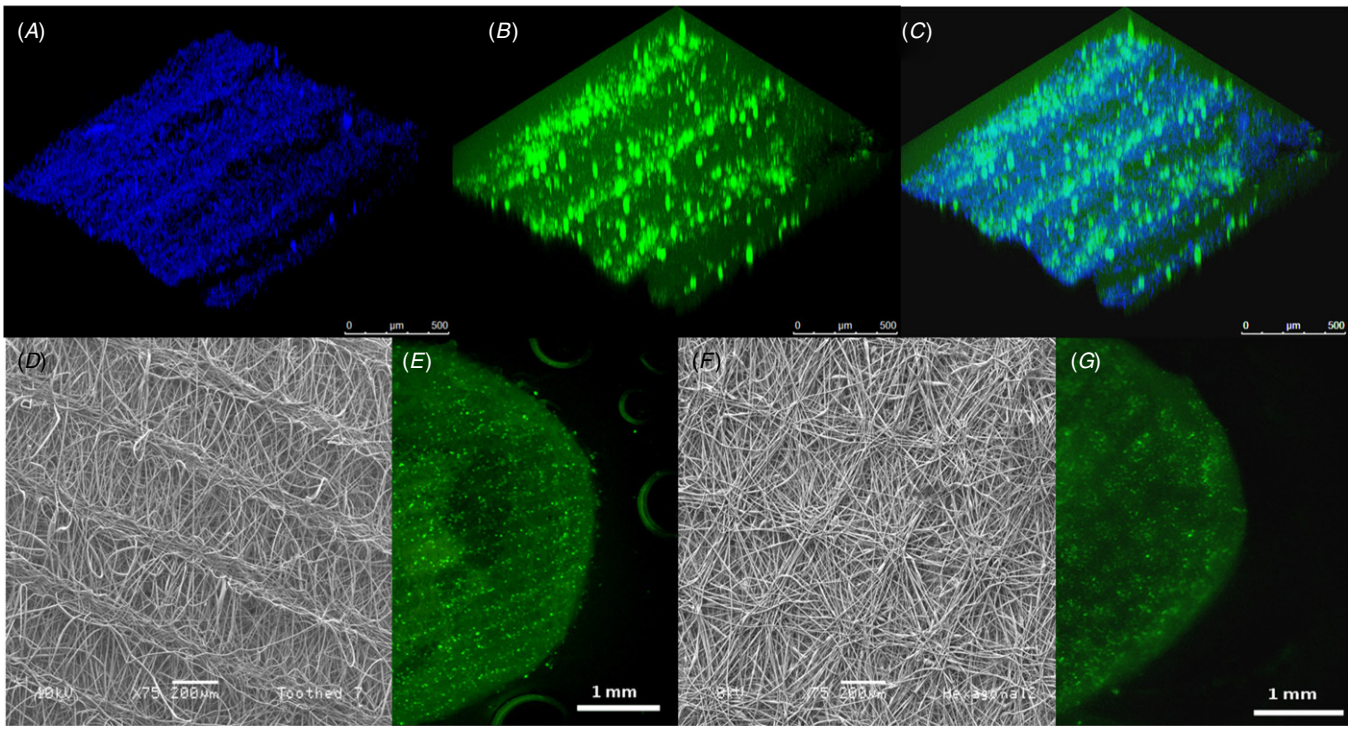

Figure 5. Analysis of mammalian cell adhesion to the patterned electrospun scaffolds. Representative macro-confocal images illustrating the 3D patterning of the sinusoidal scaffolds (*A*), the linear arrangement of the seeded eGFP-labelled 3T3 fibroblasts (*B*) and combined images confirming the adhesion of the cells to the patterned features of the scaffold (*C*). In the images the PLGA fibres are blue (reflectance) and the cells are green (GFP). Further evidence of scaffold patterning influencing cell adhesion can be seen in low magnification fluorescence imaging for both the sinusoidal (*D*) and (*E*) and hexagonal (*F*) and (*G*) patterned scaffolds as compared with representative SEM images of the fibre mats.

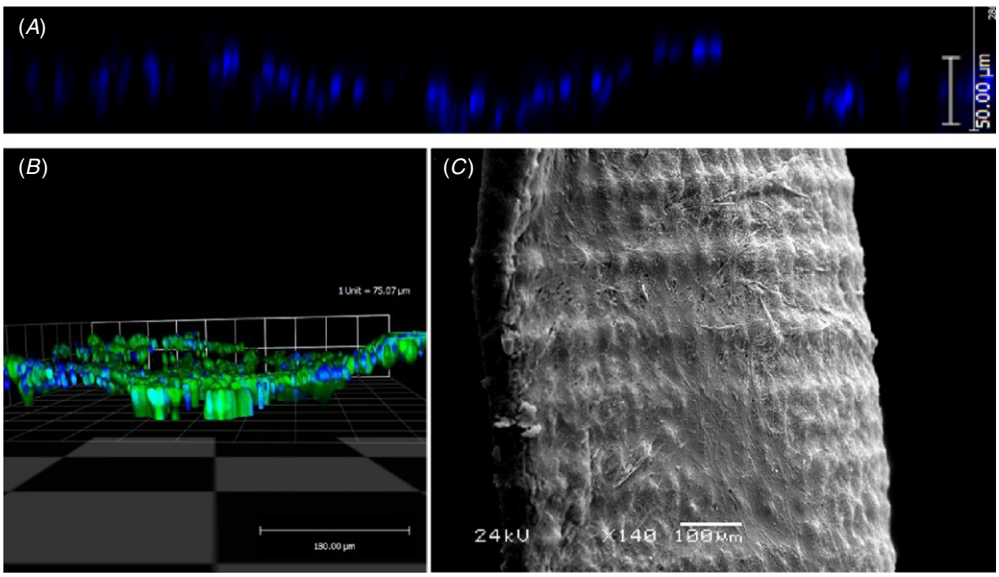

Figure 6. Analysis of mammalian cell proliferation over the patterned electrospun scaffolds. Representative micro-confocal and SEM images illustrating that the eGFP-labelled 3T3 fibroblasts proliferated along the waves of the sinusoidal scaffolds (*A*) and (*B*) reaching confluence on the patterned fibres (*C*) such that they were now held in the 3D undulating microgeometry of the scaffold. In the fluorescence micro-confocal images, the cell nuclei are blue (DAPI) and the cytoplasm green (GFP).

structure were reflected in the parameters of the sinusoidal scaffolds and are the reason why these scaffolds were the focus for cell adhesion and proliferation studies. Following seeding, the eGFP-labelled 3T3 fibroblasts were seen to preferentially adhere to the dense regions of the patterned microfibres. By the end of the culture period, the cells had proliferated over the sinusoidal waves and were held in the overall 3D undulating pattern of the scaffold. Cells were viable over the culture period and were seen to cover the surface of the scaffold structure. Although we saw no evidence of cell penetration

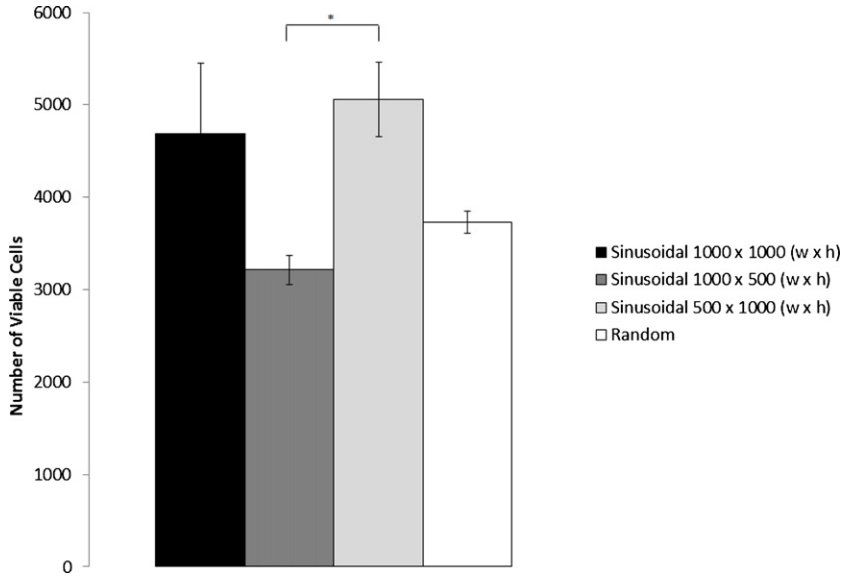

Figure 7. The number of viable cells adherent to the scaffolds was assessed using the Alamar Blue® assay following four days of culture. No difference in the number of viable cells was observed between the patterned and control (random fibres) PLGA scaffolds. Significant difference in the number of viable cells present was seen with differing sinusoidal wave height (error bars represent SEM, $n = 9$; $p < 0.05$).

into the scaffold, this was a desirable feature for the intended application of developing an *in vitro* model of the dermal papillae where a basement membrane structure was required. Should cell penetration be required for a tissue engineering application, the electrospinning conditions could be altered to fabricate a more porous structure which would allow cell migration. We found that the former pattern was transferred to the scaffold when both dense and sparse fibre mats were produced. These are the first findings to show the influence of sinusoidal electrospun scaffolds on *in vitro* cell behaviour and supports previous studies in which patterned silicon, titanium and resin constructs demonstrated that topological surfaces can be used to control both adhesion and direction of cellular migration and that 3D ridges are powerful cues for fibroblast directionality (Kaiser *et al* 2006, Curtis and Wilkinson 1997, Jeon *et al* 2010, Den Braber *et al* 1996). Using these scaffolds for the development of an *in vitro* model of the dermal papillae stem cell niche is now the focus of future work.

Conclusion

In this study, we have demonstrated for the first time that patterned hybrid electrospun scaffolds with tailored 3D micro-patterns can be manufactured using RP resin formers as templates during the electrospinning process. The PLGA fibre patterning mirrored both the geometries and dimensions of all the 3D collector designs manufactured. Using the RP method, we are able to produce simple patterns such as sinusoidal waves, as well as more complex 3D geometries such as hexagons. The Envisiontec Perfactory™ system we employed is ideally suited to the accurate production of complex microstructures and therefore holds great potential to produce a wide range of formers with controlled features, providing versatility to the end-user. Using murine 3T3 fibroblasts, we investigated the influence of the patterned geometries that mimic the 3D architecture of tissues such as skin (specifically the dermal papillae), on both mammalian cell adhesion and subsequent population of the electrospun scaffolds. The fibroblasts were found to initially adhere only to the bundles of the aligned patterned microfibres and following proliferation on the scaffolds, the sinusoidal waves of the scaffolds were able to guide the cell population to exist in a 3D microgeometry. Future work will investigate the use of such patterned fibre scaffolds to replicate tissue geometries further for use in the development of *in vitro* models for studying disease, toxicity studies and the screening of potential therapeutics. In conclusion, a novel method to fabricate electrospun scaffolds with 3D directional cues to influence cell behaviour has been developed.

Acknowledgments

The research leading to these results was supported by the Engineering and Physical Sciences Research Council (grant number EP/H028277/1) and carried out within the EPSRC Centre for Innovative Manufacturing in Regenerative Medicine. In addition, the work was supported by the European Research Council under the *European Community's* Seventh Framework Programme (FP7/2007-2013)/ERC grant agreement.

References

Bellan L M and Craighead H G 2006 Control of an electrospinning jet using electric focusing and jet steering fields *J. Vac. Sci. Technol.* B **24** 3179–84

Bisht G S, Canton G, Mirsepassi A, Kulinsky L, Oh S, Dunn-Rankin D and Madou M J 2011 Controlled continuous patterning of polymeric nanofibers on three-dimensional

substrates using low-voltage near-field electrospinning *Nano Lett.* **11** 1831–7
Brown T D, Dalton P D and Hutmacher D W 2011 Direct writing by way of melt electrospinnng *Adv. Mater.* **23** 5651–7
Brun P, Ghezzo F, Roso M, Danesin R, Palu G, Bagno A, Modesti M, Castagliuolo I and Dettin M 2011 Electrospun scaffolds of self-assembling peptides with poly(ethylene oxide) for bone tissue engineering *Acta Biomater.* **7** 2526–32
Chang C, Limkrailassiri K and Lin L 2008 Continuous near-field electrospining for large area deposition of orderly nanofiber patterns *Appl. Phys. Lett.* **93** 123111
Curtis A and Wilkinson C 1997 Topological control of cells *Biomaterials* **18** 1573–83
Dalton P D, Vaquette C, Farrugia B L, Gargaville T, Brown T D and Hutmacher D W 2013 Electrospinning and additive manufacturing: converging technologies *Biomater. Sci.* **1** 171–85
Den Braber E T, de Ruijter J E, Ginsel L A, von Recum A F and Jansen J A 1996 Quantitative analysis of fibroblast morphology on microgrooved surfaces with various groove and ridge dimensions *Biomaterials* **17** 2037–44
Dixon J E, Dick E, Rajamohan D, Shakesheff K M and Denning C 2011 Directed differentiation of human embryonic stem cells to interrogate the cardiac gene regulatory network *Mol. Ther.* **19** 1695–703
Guex A G, Birrer D L, Fortunato G, Tevaearai T and Giraud M N 2013 Anisotropically orientated electrospun matrices with an imprinted periodic micropattern: a new scaffold for engineered muscle constructs *Biomed. Mater.* **8** 021001
Jeon H, Hidai H, Hwang D J, Healy K E and Grigoropoulos C P 2010 The effect of micronscale anisotropic cross patterns on fibroblast migration *Biomaterials* **31** 4286–95
Kaiser J P, Reinmann A and Bruinink A 2006 The effect of topographic characteristics on cell migration velocity *Biomaterials* **27** 5230–41
Lee J, Lee S Y, Jang J, Jeong Y H and Cho D W 2012 Fabrication of patterned nanofibrous mats using direct-write electrospinning *Langmuir* **28** 7267–75
Li D, Ouyang G, McCann J T and Xia Y N 2005 Collecting electrospun nanofibers with patterned electrodes *Nano Lett.* **5** 913–6
Li D, Wang Y L and Xia Y N 2003 Electrospinning of polymeric and ceramic nanofibers as uniaxially aligned arrays *Nano Lett.* **3** 1167–71
Li D, Wang Y L and Xia Y N 2004 Electrospinning nanofibers as uniaxially aligned arrays and layer-by-layer stacked films *Adv. Mater.* **16** 361–3
Lyons J, Li C and Ko F 2004 Melt-electrospinning part I: processing parameters and geometric properties *Polymer* **45** 7595–603
Neves N M, Campos R, Pedro A, Cunha J, Macedo F and Reis R L 2007 Patterning of polymer nanofiber meshes by electrospinning for biomedical applications *Int. J. Nanomed.* **2** 433–48
Reneker D H and Chun I 1996 Nanometre diameter fibres of polymer produced by electrospinning *Nanotechnology* **7** 216–23
Rim N G, Shin C S and Shin H 2013 Current approaches to electrospun nanofibers for tissue engineering *Biomed. Mater.* **8** 014102
Teo W E, Inai R and Ramakrishna S 2011 Technological advances in electrospinning of nanofibers *Sci. Technol. Adv. Mater* **12** 1–19
van Aalst J A, Reed C R, Han L, Andrady T, Hromadka M, Bernacki S, Kolappa K, Collins J B and Loboa E G 2008 Cellular incorporation into electrospun nanofibers—retained viability, proliferation and function in fibroblasts *Ann. Plast. Surg.* **60** 577–83
Vats A, Tolley N S, Polak J M and Gough J E 2003 Scaffolds and biomaterials for tissue engineering: a review of clinical applications *Clin. Otolaryngol. Allied Sci.* **28** 165–72
Vaquette C and Cooper-White J J 2011 Increasing electrospun scaffold pore size with tailored collectors for improved cell penetration *Acta Biomater.* **7** 2544–57
Wu Y, Dong Z, Wilson S and Clark R L 2010 Template-assisted assembly of electrospun fibers *Polymer* **51** 3244–8
Xie J, MacEwan M R, Ray W R, Liu W, Siewe D Y and Xia Y 2010 Radially aligned electrospun nanofibers as dural substitutes for wound closure and tissue regeneration applications *ACS Nano* **4** 5027–36
Xin X, Hussain M and Mao J J 2007 Continuing differentiation of human mesenchymal stem cells and induced chondrogenic and osteogenic lineages in electrospun PLGA nanofiber scaffold *Biomaterials* **28** 316–25
Yang D, Lu B, Zhao Y and Xia Y 2007 Fabrication of aligned fibrous arrays by magnetic electrospinning *Adv. Mater.* **19** 3802–6
Zhang D and Chang J 2007 Patterning of electrospun fibers using electroconductive templates *Adv. Mater.* **19** 3664–7
Zhang D and Chang J 2008 Electrospinning of three-dimensional nanofibrous tubes with controllable architectures *Nano Lett.* **8** 3283–7
Zhang K, Wang X, Jing D, Yang Y and Zhu M 2009 Bionic electrospun ultrafine fibrous poly(L-lactic acid) scaffolds with a multi-scale structure *Biomed. Mater.* **4** 1–6